Electronic Supplementary Material (ESI) for MedChemComm.

Scaffold hopping from synthetic RXR modulators by virtual screening and *de novo* design

Daniel Merk[a], Francesca Grisoni[a,b], Lukas Friedrich[a], Elena Gelzinyte[a], Gisbert Schneider[a]

[a)] Department of Chemistry and Applied Biosciences, Swiss Federal Institute of Technology (ETH), Vladimir-Prelog-Weg 4, CH-8093 Zurich, Switzerland, E-mail: gisbert.schneider@pharma.ethz.ch

[b)] Department of Earth and Environmental Sciences, University of Milano-Bicocca, P.za della Scienza, 1, IT-20126 Milan, Italy

- Supporting information -

Table of contents

Supporting figure & tables

Table S1. Potential RXR modulators retrieved by virtual screening and their *in vitro* activity (results are mean±SEM, *n*=2 for inactives and *n*≥4 for actives).

structure	ID	activity: EC_{50}/IC_{50} (fold activation) RXRα	RXRβ	RXRγ
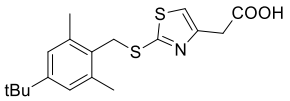	**3**	inactive (30 µM)	inactive (30 µM)	inactive (30 µM)
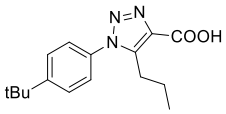	**4**	inactive (30 µM)	inactive (30 µM)	inactive (30 µM)
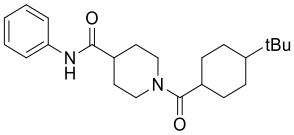	**5**	antagonist IC_{50} = 7±2 µM	antagonist IC_{50} = 10.9±0.3 µM	antagonist IC_{50} = 8.2±0.8 µM
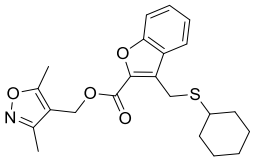	**6**	toxic (could not be characterized)	n.d.	n.d.
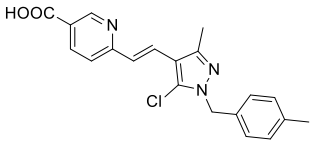	**7**	inactive (30 µM)	inactive (30 µM)	inactive (30 µM)
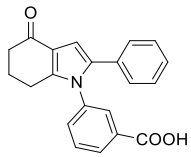	**8**	inactive (30 µM)	inactive (30 µM)	inactive (30 µM)
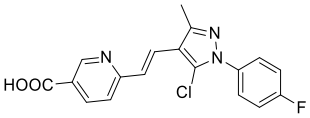	**9**	inactive (30 µM)	inactive (30 µM)	inactive (30 µM)
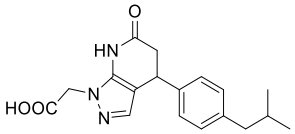	**10**	inactive (30 µM)	inactive (30 µM)	inactive (30 µM)
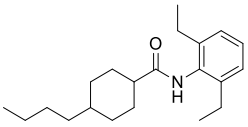	**11**	inactive (30 µM)	inactive (30 µM)	inactive (30 µM)
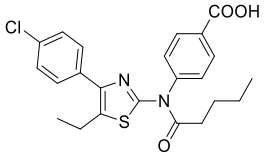	**12**	partial agonist EC_{50} = 21±1 µM (2.9±0.1-fold)	inactive (30 µM)	inactive (30 µM)
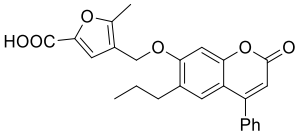	**13**	partial agonist EC_{50} = 21±3 µM (3.0±0.5-fold)	partial agonist EC_{50} = 42.3±0.3 µM (8.2±0.1-fold)	partial agonist EC_{50} = 51±9 µM (12±4-fold)
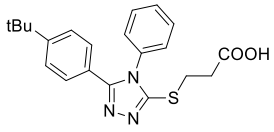	**14**	antagonist IC_{50} = 4.8±0.7 µM	antagonist IC_{50} = 12.3±0.4 µM	part. antagonist IC_{50} = 18.1±0.1 µM

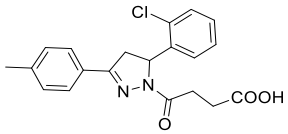	**15**	antagonist IC_{50} = 18±4 μM	antagonist IC_{50} = 6±1 μM	antagonist IC_{50} = 4.9±0.5 μM
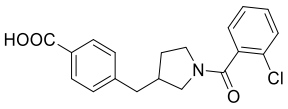	**16**	inactive (30 μM)	inactive (30 μM)	inactive (30 μM)
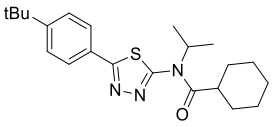	**17**	inactive (30 μM)	inactive (30 μM)	inactive (30 μM)
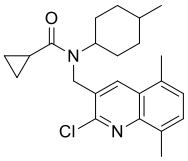	**18**	inactive (30 μM)	inactive (30 μM)	inactive (30 μM)
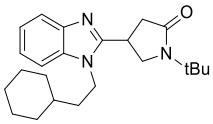	**19**	partial agonist EC_{50} = 27±3 μM (6.2±1.0-fold)	partial agonist EC_{50} = 36.6±0.2 μM (3.3±0.1-fold)	partial agonist EC_{50} = 24±6 μM (2.3±0.1-fold)

Table S2. Preliminary structure activity relationship of novel RXR antagonists: Antagonists **14** and **20**-**23** and their *in vitro* activity (results are mean±SEM, *n*=2 for inactives and *n*≥4 for actives).

structure	ID	IC_{50}		
		RXRα	RXRβ	RXRγ
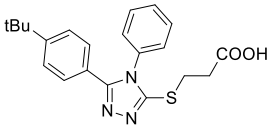	**14**	4.8±0.7 μM	12.3±0.4 μM	18.1±0.1 μM
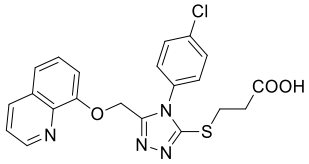	**20**	inactive (30 μM)	inactive (30 μM)	inactive (30 μM)
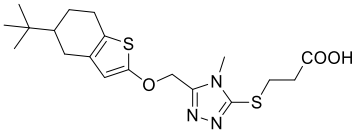	**21**	2.0±0.8 μM	18±2 μM	1.78±0.03 μM
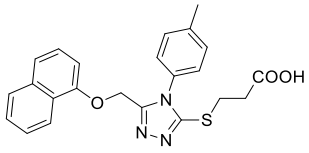	**22**	12±7 μM	14±4 μM	17±8 μM
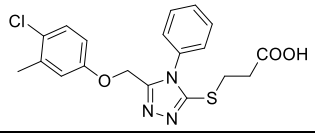	**23**	12±4 μM	11±2 μM	18.3±0.3 μM

Table S3. AlogP and AlogS values of novel RXR modulators

ID	**5**	**12**	**13**	**14**	**15**	**19**	**21**	**22**	**23**	**24**	**25**	**26**
AlogP	4.92	5.69	4.98	4.37	3.40	5.88	3.72	3.93	3.39	6.27	3.93	3.66
AlogS	-4.76	-5.79	-4.71	-4.92	-4.80	-4.76	-4.14	-5.00	-4.61	-6.18	-4.02	-3.27

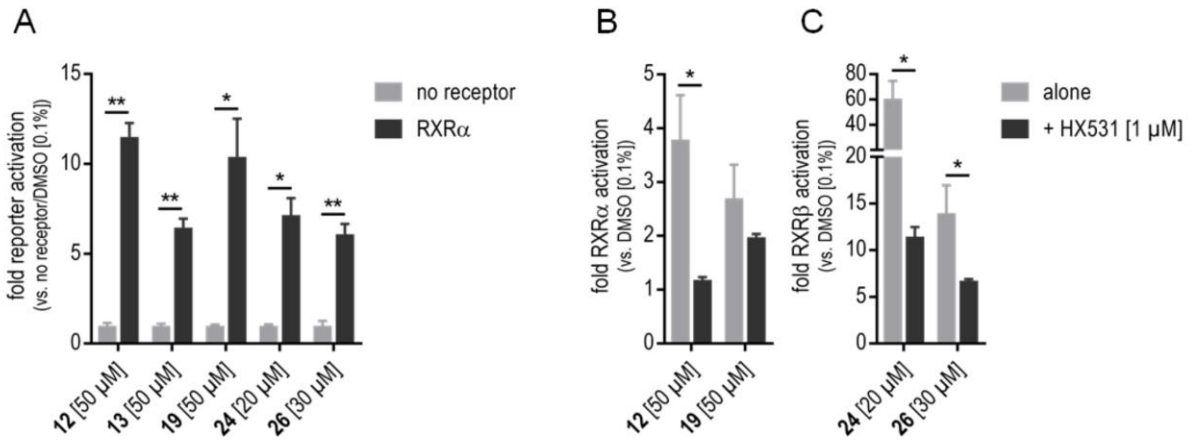

Figure S1: Control experiments confirmed RXR mediated activity of agonistic RXR modulators **12**, **13**, **19**, **24** and **26**: (A) No reporter transactivation by **12**, **13**, **19**, **24** and **26** (20, 30 or 50 µM) was observed in absence of a Gal4-hybrid receptor (light grey bars) whereas significant reporter transactivation occurred in presence of the Gal4-RXRα hybrid receptor (dark grey bars). (B) RXRα activating effects of **12** and **19** (50 µM, light grey bars) could be blocked by addition of the RXR antagonist HX531 (1 µM, dark grey bars). (C) RXRβ activating effects (light grey bars) of **24** (20 µM) and **26** (30 µM) could be blocked by addition of the RXR antagonist HX531 (1 µM, dark grey bars). $n = 3$ in (A) and $n = 4$ in (B) and (C). * $p < 0.05$; ** $p < 0.01$; *** $p < 0.001$.

Notes: RXRβ was selected for the antagonistic control experiments of **24** and **26** since the compounds are significantly more active on this subtype. Inhibition of RXR activating effects of **13** (50 µM) by HX531 (1 µM) could not be studied because their combination resulted in too high toxicity.

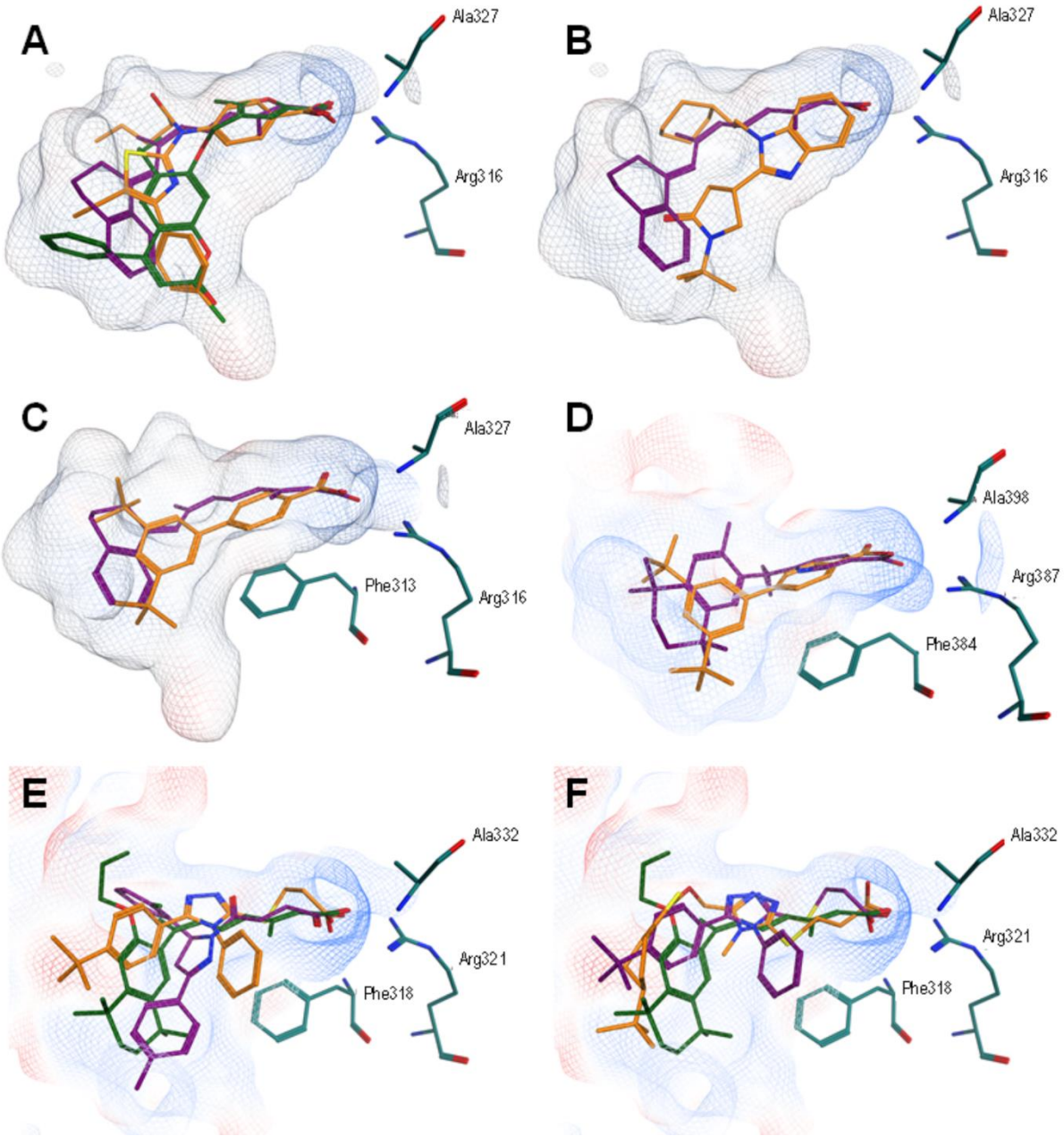

Figure S2. *Molecular docking (A-C: RXRα; D: RXRβ; E&F: mRXRα)*: (A) Partial agonists **12** (orange) and **13** (green) despite their structural diversity form similar binding modes with the RXRα (PDB-ID: 4K4J[1]) ligand binding site and neutralize Arg_{336} as the co-crystallized ligand (purple). (B) The non-acidic modulator **19** (orange) does not interact with Arg_{336} and differs from the co-crystallized ligand (purple) in its binding mode. Proposed binding modes of **24** in RXRα (C) and RXRβ (D) are similar and cannot explain subtype preferential activity. (E) Antagonists **15** (purple) covers the ligand binding site in mRXRα (PDB-ID: 3A9E[2]) similar to the co-crystalized ligand (green) whereas for **14** (orange) a π-stacking contact with Phe318 is suggested but the compound does not fill the hydrophobic end of the binding pocket. (F) The elongated lipophilic backbone of antagonist **21** (orange) fills the hydrophobic end of the pocket better than **14** (purple) but lacks π-stacking with Phe318.

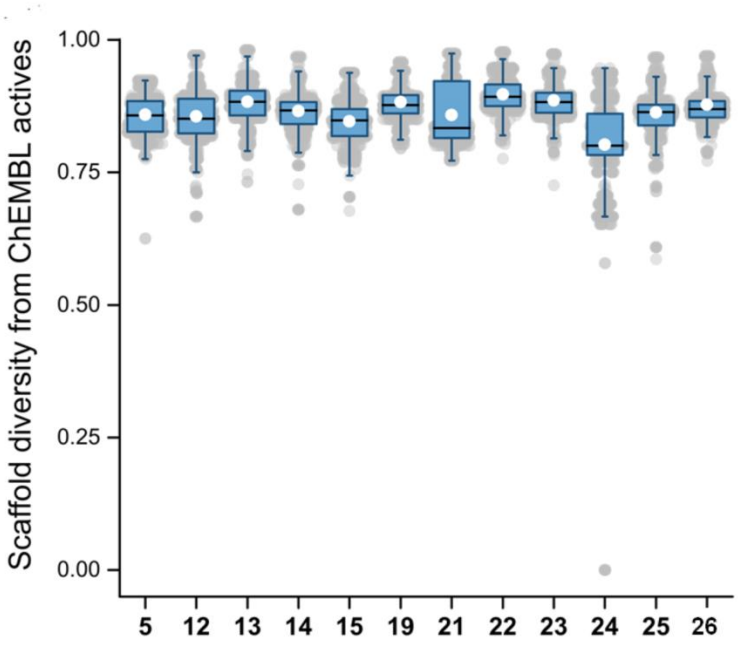

Figure S3: *Diversity of novel RXR modulators*: Comparison of scaffolds in newly identified RXR modulators to ChEMBL annotated RXR agonists and antagonists (IC/EC_{50} < 50 µM, *n* = 521) in terms of Jaccard-Tanimoto distance calculated on the scaffolds' fragments (Extended Connectivity Fingerprints[8], radius = 0 to 4 bonds, bits = 1024): All new RXR modulator chemotypes are markedly different to known modulators.

Materials & Methods

Computational methods

Structure preparation

The commercially available screening libraries of ChemBridge, Asinex, Enamine and Specs as well as reference compounds were washed and protonated with MOE (version 2016.08) at pH7.

Distance calculation and ranking using the CATS[3] descriptors

The CATS2 descriptors were calculated for the screening compounds collection and the reference compounds using in-house software (up to a topological distance of 10 bonds). Euclidean distance calculations of all screening compounds to the three reference compounds were performed using in-house software. All screening compounds were then ranked according to their distance to the query compounds and compounds ranked in the top 100 positions for each query were included. In addition, compounds were ranked according to the sum of their ranks for individual queries and compounds ranked in the top 100 positions were considered.

Macromolecular target prediction (SPiDER)[4]

For the entire screening library, the CATS2 descriptor (see above) and the set of two-dimensional MOE descriptors (MOE descriptors KNIME node; MOE2016.08; forcefield: MMFF94*) were calculated and all compounds were individually placed on two pre-trained self-organizing maps for target prediction (SPiDER). The results were filtered for compounds predicted to be active on retinoid X receptor with a *p*-value < 0.05 and compounds were ranked according to their p-value. Compounds ranked in the top 100 positions were considered.

Virtual screening for antagonists using the CATS descriptors, fingerprints and the LIQUID descriptors[5]

The CATS (up to a topological distance of 10 bonds) and LIQUID descriptors were calculated using in-house software for the screening compounds collection after pre-filtering for 1,2,3-substituted five-ring systems as well as for the reference antagonists. Morgan fingerprints (1024 bits, radius = 0-2) for the same sets of compounds were calculated using RDKit. Euclidean distance of the pre-filtered screening compounds to the three reference antagonists for CATS and LIQUID descriptor as well as Tanimoto similarity for fingerprints were calculated. The screening compounds were then ranked according to their distance/similarity to each query compound and compounds ranked at least twice in the top 5 positions were included.

De-novo design (Design of Genuine Structures)[6]

De novo designs were generated by reaction-driven de-novo design using DOGS (Design of Genuine Structures) with seven RXR agonists from literature or our in-house library as templates. For each template, one DOGS run was performed (preferences: starting fragments: 100, ISOAK-alpha: 0.40, including reduced graph abstraction level) and the de-novo designs resulting from each individual run were ranked according to Euclidean distances calculated on CATS2 and SPIDER *p*-values as described above. **24**-**26** were selected taking into account their design frequency from different templates, individual ranks and building block availability.

Scaffold diversity analysis

Bemis-Murcko scaffolds[7] were computed using RDKit module of python (v 2.7). Extended Connectivity Fingerprints[8] (radius = 0 to 4 atoms, 1024 bit) were computed with Dragon 7[9] using the scaffolds' SMILES as input. The scaffold diversity between active hits and of ChEMBL annotated actives was determined using the Jaccard-Tanimoto index calculated on ECFPs, computed in a MATLAB environment[10].

Molecular docking

The crystal structures of the human retinoid X receptor α (PDB-ID: 4K4J[1]) and β (PDB-ID: 1H9U[11]), and mouse RXR alpha (PDB code 3A9E[2]) were prepared with QuickPrep in MOE2016.08. The molecular structure was protonated at pH 7. Structural issues were corrected (adding hydrogens,

capping C terminus and loop from Pro244-Asn262). Water molecules farther away than 4.5 Å from the receptor or ligand were deleted. The positions of receptor atoms were restrained (force constant = 10, buffer = 0.25 Å). The position of all atoms farther away than 8 Å from the ligand were fixed, except hydrogen atoms close to the ligand. The resulting structure was minimized in the AMBER10:EHT (Extended Hückel Theory) forcefield (termination value = 0.1 kcal mol^{-1} $Å^{-1}$).

Hydrogens were added to all ligand compounds, ligand structures were protonated at pH 7 and all structures were minimized in the AMBER10:EHT (Extended Hückel Theory) forcefield (termination value = 0.1 kcal mol^{-1} $Å^{-1}$).

Docking of ligands was executed in MOE2016.08 using the integrated GOLD[12] docking program as placement method. The active site was defined by ligand atoms of the co-crystalized ligand. The efficiency of the docking calculation was set to “Very Flexible” (200%). For all other GOLD-specific docking options the default settings were used. The fitness function “GOLDscore” was used as scoring method. 100 Poses of each ligand were generated. The “Induced Fit” method was selected for the further refinement of the poses using the standard parameters. The GBVI/WSA dG scoring was chosen as final scoring function. 10 final poses of each ligand were retained.

Calculation of AlogP and AlogS

AlogP and AlogS values were calculated using the ALOGPS 2.1[13] online tool.

Chemistry

General

All chemicals and solvents were reagent grade and used without further purification, unless specified otherwise. All reactions were conducted in oven-dried glassware under argon-atmosphere and in absolute solvents. NMR spectra were recorded on a Bruker AV 400 spectrometer (Bruker Corporation, Billerica, MA, USA). Chemical shifts (δ) are reported in ppm relative to TMS as reference; approximate coupling constants (J) are shown in Hertz (Hz). Mass spectra were obtained on an Advion expression CMS (Advion, Ithaka, NY, USA) equipped with an Advion plate express TLC extractor (Advion) using electrospray ionization (ESI). High-resolution mass spectra were recorded on a Bruker maXis ESI-Qq-TOF-MS instrument (Bruker). Compound purity was analyzed on a Varian ProStar HPLC (SpectraLab Scientific Inc., Markham, ON, Canada) equipped with a MultoHigh100 Phenyl 5 µ 240+4 mm column (CS-Chromatographie Service GmbH, Langerwehe, Germany) using a gradient (H_2O/MeOH 80:20+0.1% formic acid isocratic for 5 min to MeOH+0.1% formic acid after additional 45 min and MeOH+0.1% formic acid for additional 10 min) at a flow rate of 1 ml/min and UV-detection at 245 nm and 280 nm. All final compounds for biological evaluation had a purity > 95% (area-under-the-curve for UV_{245} and UV_{280} peaks).

3',5'-Di-tert-butyl-[1,1'-biphenyl]-4-carboxylic acid (**24**): 1-Bromo-3,5-di-*tert*-butylbenzene (**28**, 135 mg, 0.50 mmol, 1.00 eq) and 4-boronobenzoic acid (**29**, 108 mg, 0.65 mmol, 1.30 eq) were dissolved in a mixture of toluene (abs., 9 ml) and ethanol (abs., 1 ml), caesium carbonate (488 mg, 1.50 mmol, 3.00 eq) was added and the mixture was stirred at room temperature for 30 min. Tetrakis(triphenylphosphin)palladium (29 mg, 0.025 mmol, 0.05 eq) was added and the mixture was stirred under reflux for 6 h. After cooling to room temperature, 25 ml 10% aqueous hydrochloric acid were added, and the mixture was extracted three times with 25 ml ethyl acetate at a time. The combined organic layers were dried over magnesium sulfate and the solvents were evaporated in vacuum. The crude product was purified by column chromatography using hexane/ethyl acetate/acetic acid (89:9:2) as mobile phase to yield the title compound as colorless solid (64 mg, 41%). ^{1}H NMR (400 MHz, acetone-d_6): δ = 1.26 (s, 18H), 7.42 – 7.45 (m, 3H), 7.64 – 7.71 (m, 2H), 7.95 – 8.01 (m, 2H), 11.09 (s, 1H) ppm. ^{13}C NMR (101 MHz, acetone-d_6): δ = 30.87, 34.69, 121.53, 122.22, 127.18, 130.10, 139.36, 143.42, 146.59, 151.36, 166.61 ppm. MS (ESI-): *m/z* 309.19 $[M-H]^-$. HRMS (ESI-): *m/z* calculated 309.1860 for $C_{21}H_{25}O_2$ found 309.1858 $[M-H]^-$.

3-(5-([1,1'-Biphenyl]-4-yl)oxazol-2-yl)propanoic acid (**25**): 3-(5-(4-Chlorophenyl)oxazol-2-yl)propanoic acid (**30**, 126 mg, 0.50 mmol, 1.00 eq) and phenylboronic acid (**31**, 79 mg, 0.65 mmol, 1.30 eq) were dissolved in toluene (abs., 10 ml), caesium carbonate (488 mg, 1.50 mmol, 3.00 eq) was added and the mixture was stirred at room temperature for 30 min. [1,1′-bis(diphenylphosphino)ferrocene]dichloropalladium(II) (37 mg, 0.05 mmol, 0.10 eq) was added and the mixture was stirred under reflux for 24 h. After cooling to room temperature, 25 ml 10% aqueous hydrochloric acid were added, and the mixture was extracted three times with 25 ml ethyl acetate at a time. The combined organic layers were dried over magnesium sulfate and the solvents were evaporated in vacuum. The crude product was purified by column chromatography using methylene chloride/methanol (96:4) as mobile phase to yield the title compound as colorless solid (45 mg, 31%). ^{1}H NMR (500 MHz, DMSO-d_6): δ = 2.77 (t, *J* = 7.0 Hz, 2H), 3.05 (t, *J* = 7.0 Hz, 2H), 7.39 (t, *J* = 7.4 Hz, 1H), 7.50 (dd, *J* = 10.5, 4.8 Hz, 2H), 7.60 (d, *J* = 5.4 Hz, 1H), 7.75 – 7.70 (m, 2H), 7.82 – 7.75 (m, 4H), 12.34 (s, 1H) ppm. ^{13}C NMR (126 MHz, DMSO): δ = 23.51, 30.75, 123.11, 124.73, 127.03, 127.17, 127.72, 128.22, 129.49, 139.74, 140.17, 150.42, 163.59, 173.64. MS (ESI-): *m/z* 292.21 $[M-H]^-$. HRMS (MALDI): *m/z* calculated 294.1133 for $C_{17}H_{16}ClN_2O_2$ found 294.1129 $[M+H]^+$.

1-(3-Chlorophenyl)-5-(2,5-dimethyl-1H-pyrrol-1-yl)-1H-pyrazole-4-carbonitrile (**26**): 5-Amino-1-(3-chlorophenyl)-1*H*-pyrazole-4-carbonitrile (**32**, 109 mg, 0.50 mmol, 1.00 eq) and hexane-2,5-dion (**33**, 63 mg, 0.55 mmol, 1.10 eq) were dissolved in methylene chloride (10 ml), montmorillonite K10 (0.5 g) was added and the mixture stirred at room temperature for 15 minutes before the solvent was evaporated under reduced pressure. The dry powder mixture was transferred to a microwave vial and irradiated to 90°C for 30 minutes. The powder was then suspended in ethyl acetate (25 ml) and montmorillonite K10 was filtered off. The resulting solution was washed with 5% aqueous hydrochloric acid and brine, and dried over magnesium sulfate. The solvent was evaporated under reduced

pressure and the crude product was purified by column chromatography using methylene chloride/methanol (98:2) as mobile phase to yield the title compound as yellow solid (132 mg, 89%). ^{1}H NMR (400 MHz, acetone-d_6): δ = 1.84 (s, 6H), 5.89 (s, 2H), 6.87 – 6.96 (m, 2H), 7.29 – 7.38 (m, 2H), 8.28 (s, 1H) ppm. ^{13}C NMR (101 MHz, acetone-d_6): δ = 11.26, 109.50, 111.34, 120.00, 120.15, 121.86, 128.50, 129.08, 131.06, 134.59, 142.76 ppm. MS (ESI+): *m/z* 297.09 $[M+H]^+$. HRMS (ESI+): *m/z* calculated 297.0902 for $C_{16}H_{14}ClN_4$ found 297.0893 $[M+H]^+$.

In vitro pharmacological methods

Hybrid reporter gene assays for RXRα, RXRβ and RXRγ

Plasmids: The Gal4-fusion receptor plasmids pFA-CMV-hRXRα-LBD[14], pFA-CMV-hRXRβ-LBD[14] and pFA-CMV-hRXRγ-LBD[14] coding for the hinge region and ligand binding domain (LBD) of the canonical isoform of the respective nuclear receptor have been reported previously. pFR-Luc (Stratagene) was used as reporter plasmid and pRL-SV40 (Promega) for normalization of transfection efficiency and cell growth.

Assay procedure: HEK293T cells were grown in DMEM high glucose, supplemented with 10% FCS, sodium pyruvate (1 mM), penicillin (100 U/mL) and streptomycin (100 µg/mL) at 37 °C and 5% CO_2. The day before transfection, HEK293T cells were seeded in 96-well plates ($2.5 \cdot 10^4$ cells/well). Before transfection, medium was changed to Opti-MEM without supplements. Transient transfection was carried out using Lipofectamine LTX reagent (Invitrogen) according to the manufacturer's protocol with pFR-Luc (Stratagene), pRL-SV40 (Promega) and pFA-CMV-h*NR*-LBD. 5 h after transfection, medium was changed to Opti-MEM supplemented with penicillin (100 U/mL), streptomycin (100 µg/mL), now additionally containing 0.1% DMSO and the respective test compound or 0.1% DMSO alone as untreated control. Each concentration was tested in triplicates and each experiment was repeated independently at least three times. Following overnight (12-14 h) incubation with the test compounds, cells were assayed for luciferase activity using Dual-Glo™ Luciferase Assay System (Promega) according to the manufacturer's protocol. Luminescence was measured with an Infinite M200 luminometer (Tecan Deutschland GmbH). Normalization of transfection efficiency and cell growth was done by division of firefly luciferase data by renilla luciferase data and multiplying the value by 1000 resulting in relative light units (RLU). Fold activation was obtained by dividing the mean RLU of a test compound at a respective concentration by the mean RLU of untreated control. Relative activation was obtained by dividing the fold activation of a test compound at a respective concentration by the fold activation of the reference agonist bexarotene at 1 µM. All RXR hybrid assays were validated with the above-mentioned reference agonist which yielded EC_{50} values in agreement with literature. The assay was repeated in absence of a hybrid receptor by only transfecting reporter gene construct and control gene for all agonistic and partial agonistic compounds as control experiment to confirm nuclear receptor mediated activity.

NMR spectra & HPLC traces of compounds 24-26

Compound **24**

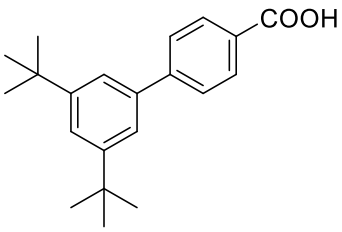

^{1}H-NMR

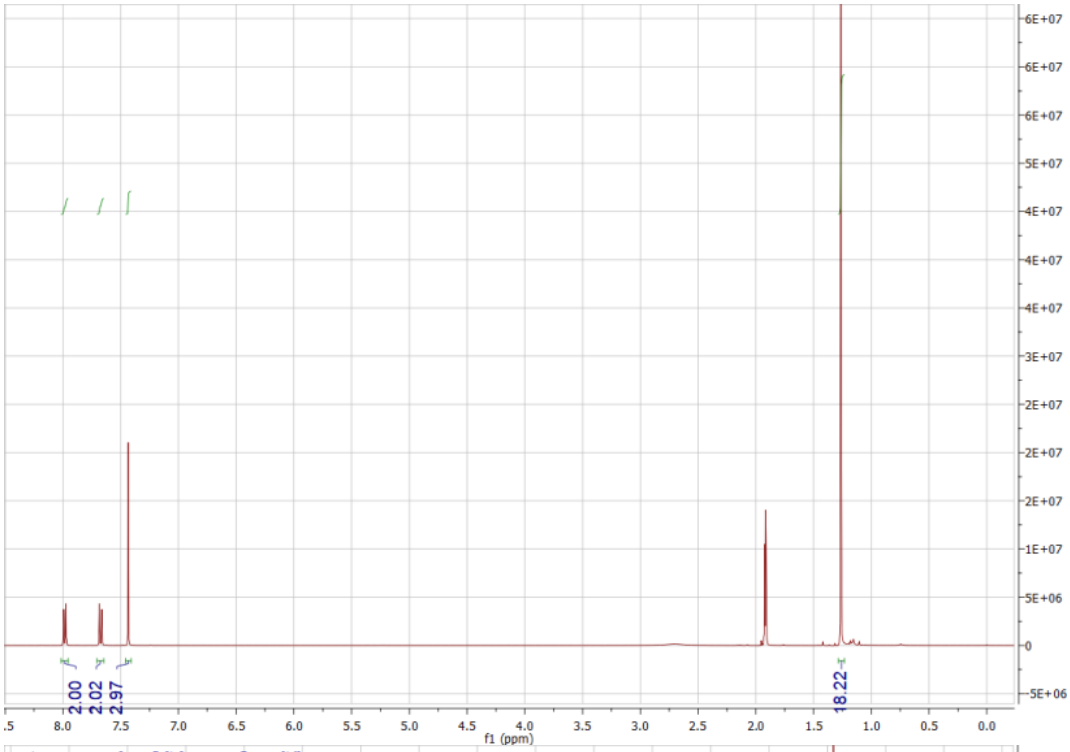

^{13}C-NMR

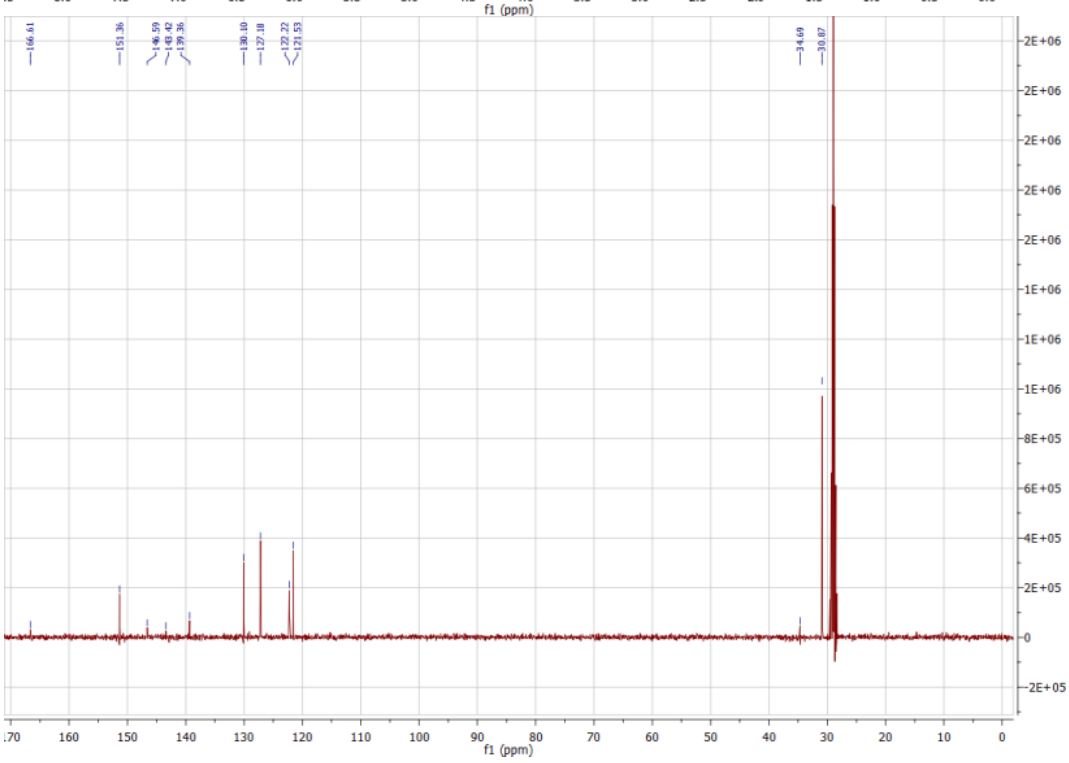

HPLC
245 nm

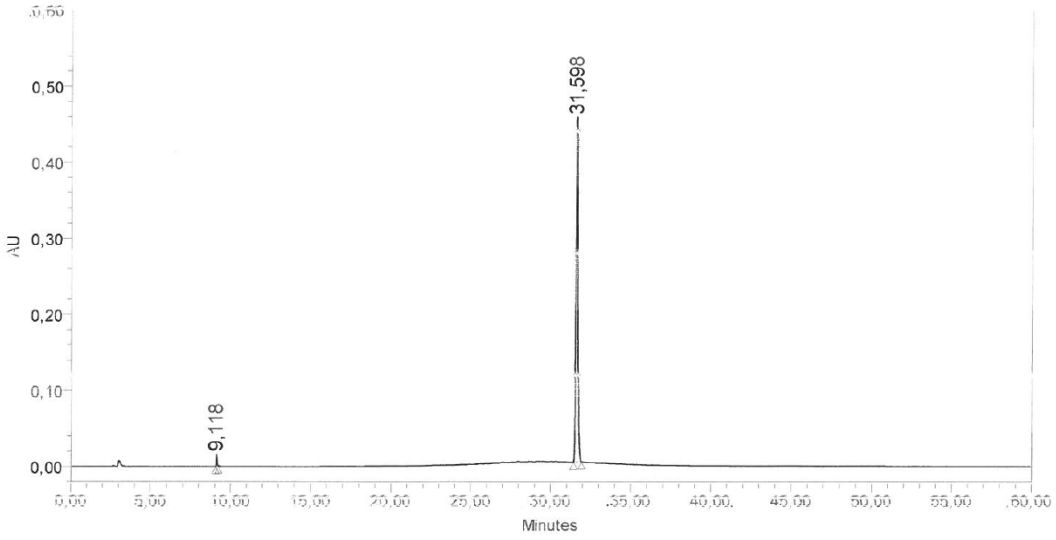

	RT	Area	% Area	Height
1	9,118	51259	1,35	15570
2	31,598	3752638	98,65	453311

HPLC
280 nm

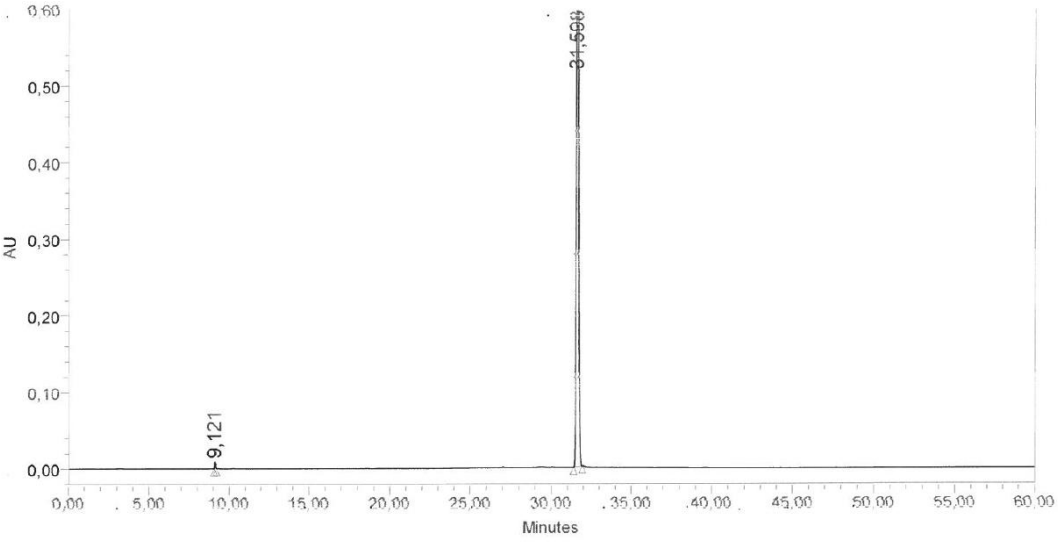

	RT	Area	% Area	Height
1	9,121	32053	0,42	9032
2	31,598	7594714	99,58	903751

Compound **25**

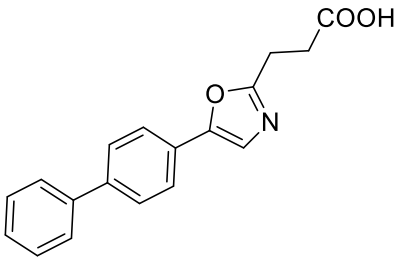

^{1}H-NMR

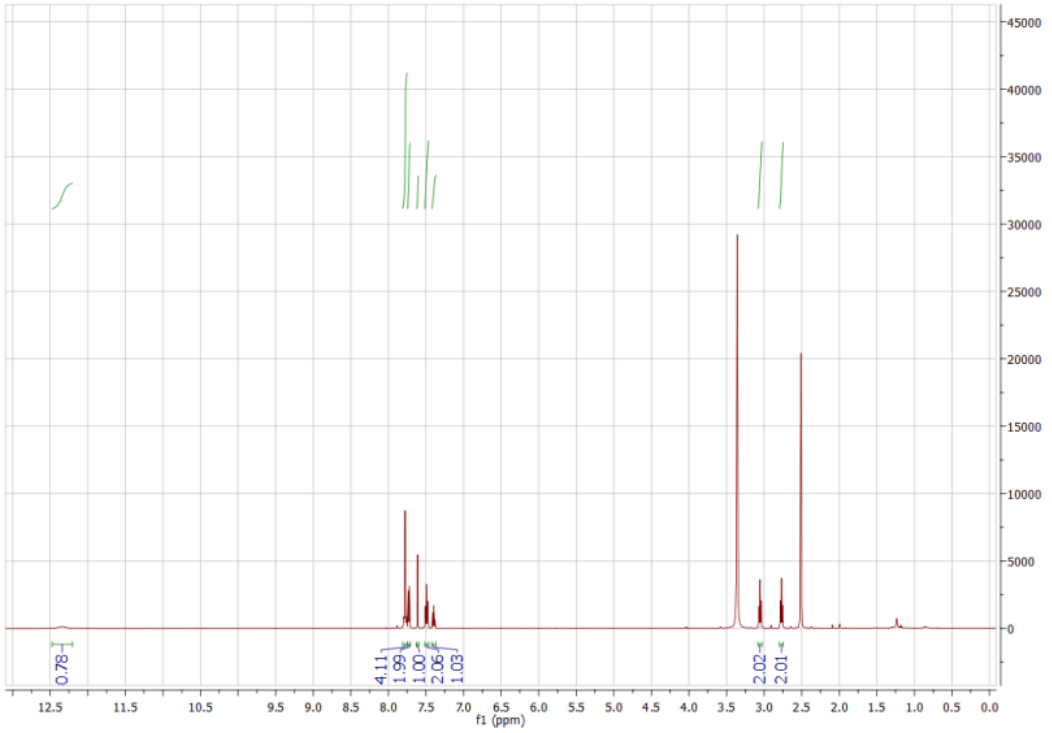

^{13}C-NMR

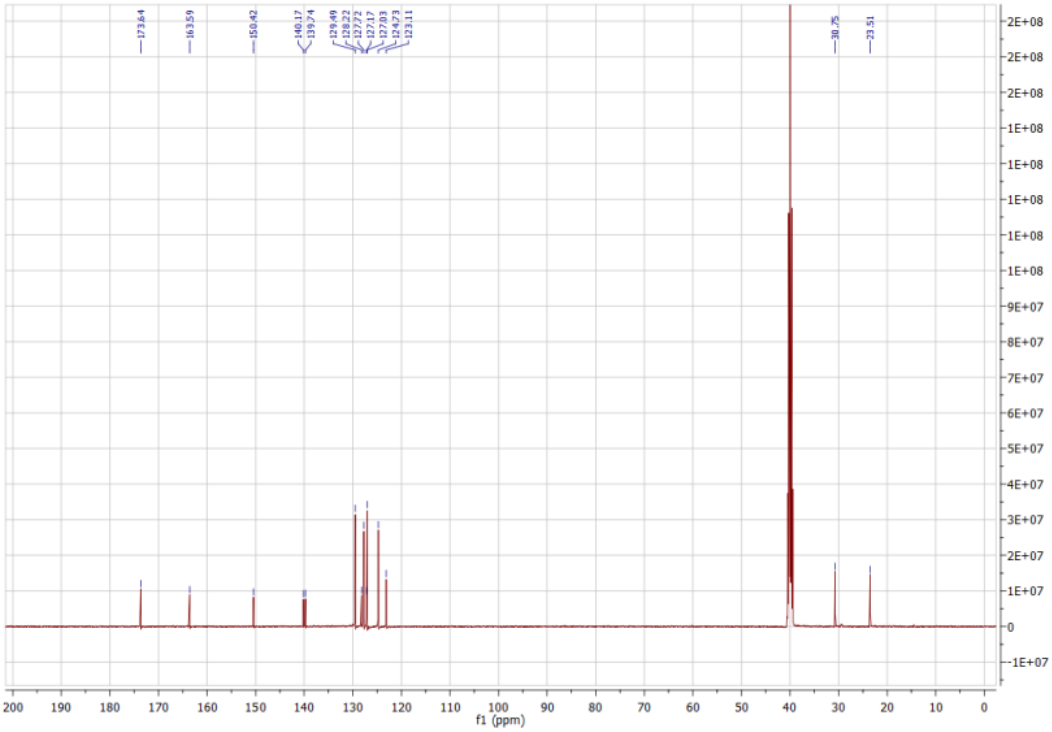

HPLC
245 nm

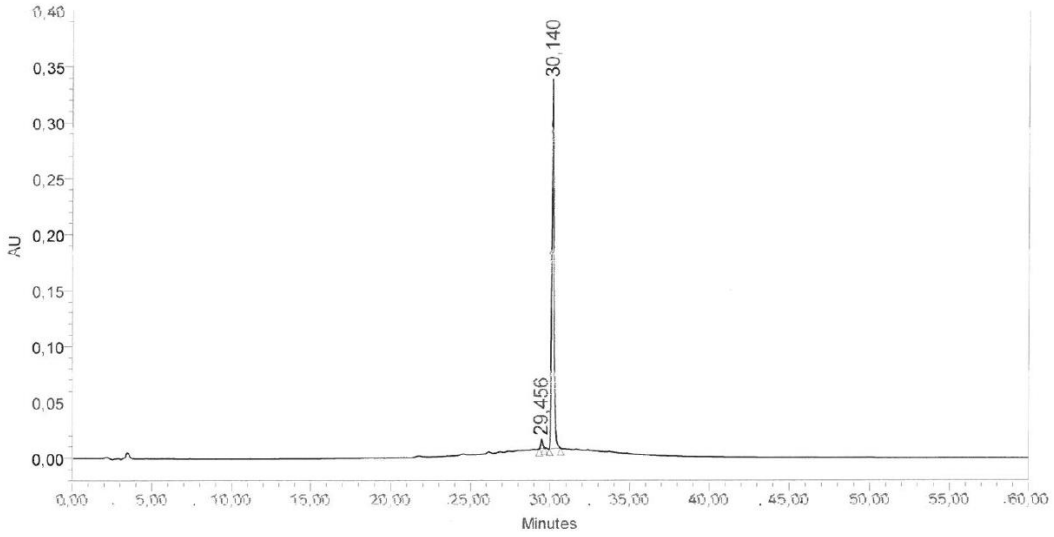

	RT	Area	% Area	Height
1	29,456	71995	2,19	8229
2	30,140	3215132	97,81	331810

HPLC
280 nm

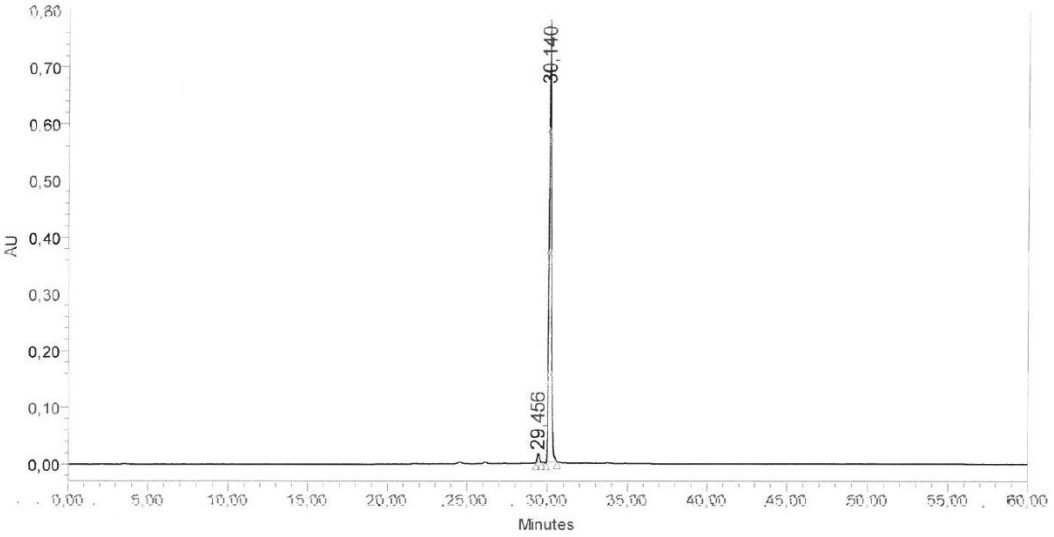

	RT	Area	% Area	Height
1	29,456	143161	1,85	16194
2	30,140	7607774	98,15	783712

Compound **26**

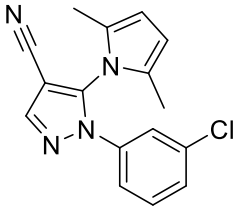

^{1}H-NMR

^{13}C-NMR

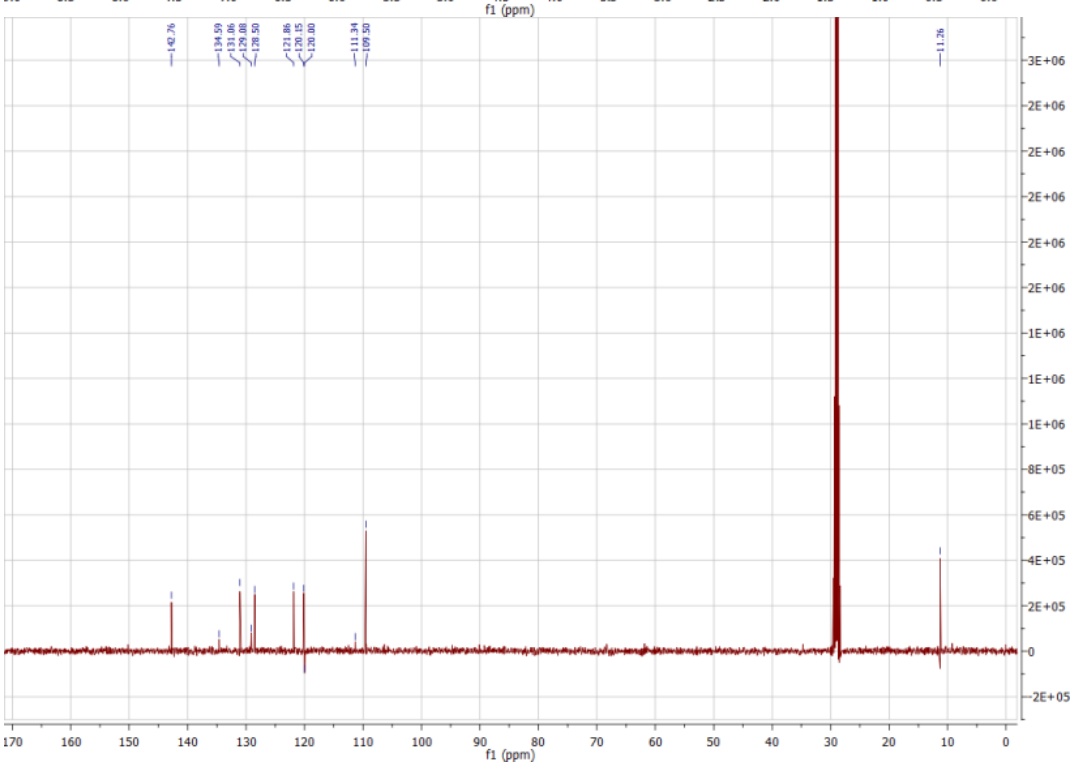

HPLC
245 nm

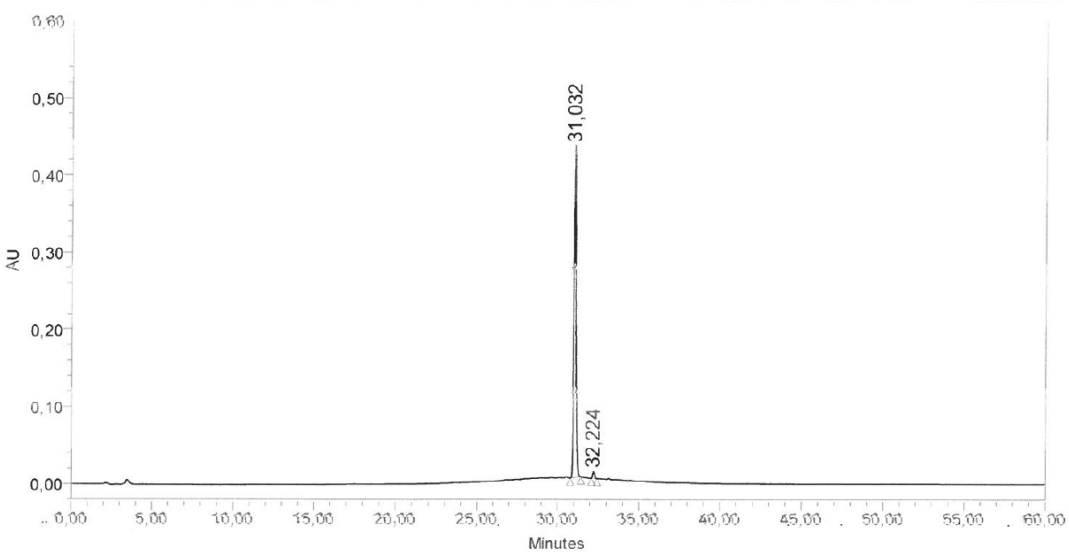

	RT	Area	% Area	Height
1	31,032	3875859	98,14	429932
2	32,224	73606	1,86	8972

HPLC
280 nm

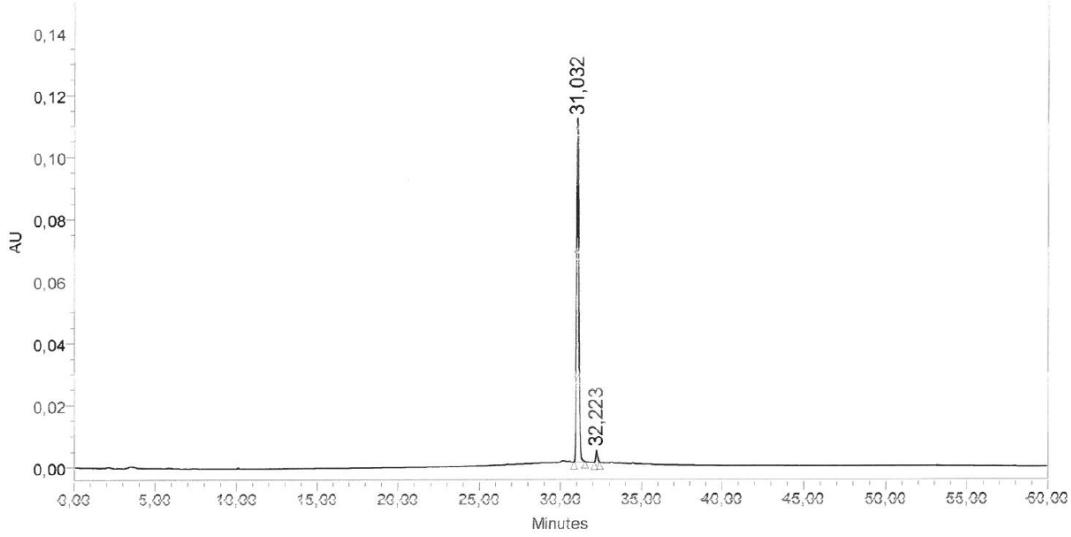

	RT	Area	% Area	Height
1	31,032	1009406	96,93	110522
2	32,223	31924	3,07	3891

Supporting References

1 L. J. Boerma, G. Xia, C. Qui, B. D. Cox, M. J. Chalmers, C. D. Smith, S. Lobo-Ruppert, P. R. Griffin, D. D. Muccio and M. B. Renfrow, *J. Biol. Chem.*, 2014, **289**, 814.

2 Y. Sato, N. Ramalanjaona, T. Huet, N. Potier, J. Osz, P. Antony, C. Peluso-Iltis, P. Poussin-Courmontagne, E. Ennifar, Y. Mély, A. Dejaegere, D. Moras and N. Rochel, *PLoS One*, 2010, **5**, e15119.

3 M. Reutlinger, C. P. Koch, D. Reker, N. Todoroff, P. Schneider, T. Rodrigues and G. Schneider, *Mol. Inf.*, 2013, **32**, 133.

4 D. Reker, T. Rodrigues, P. Schneider and G. Schneider, *Proc. Natl. Acad. Sci. U. S. A.*, 2014, **111**, 4067.

5 Y. Tanrikulu, M. Nietert, U. Scheffer, E. Proschak, K. Grabowski, P. Schneider, M. Weidlich, M. Karas, M. Göbel and G. Schneider, *ChemBioChem*, 2007, **8**, 1932.

6 M. Hartenfeller, H. Zettl, M. Walter, M. Rupp, F. Reisen, E. Proschak, S. Weggen, H. Stark and G. Schneider, *PLoS Comput. Biol.*, 2012, **8**, e1002380.

7 G. W. Bemis and M. A. Murcko, *J. Med. Chem.*, 1996, **39**, 2887.

8 D. Rogers and M. Hahn, *J. Chem. Inf. Model.*, 2010, **50**, 742.

9 H. kode-solutions.net., Kode srl., Dragon (software for molecular descriptor calculation) version 7.0.6, 2016.

10 MATLAB 2017a, U. S. The MathWorks, Inc., Natick, Massachusetts.

11 J. D. Love, J. T. Gooch, S. Benko, C. Li, L. Nagy, V. K. K. Chatterjee, R. M. Evans and J. W. R. Schwabe, J. *Biol. Chem.*, 2002, **277**, 11385.

12 G. Jones, P. Willett, R. C. Glen, A. R. Leach and R. Taylor, *J. Mol. Biol.*, 1997, **267**, 727.

13 I. V Tetko and V. Y. Tanchuk, *J. Chem. Inf. Comput. Sci.*, 2002, **42**, 1136.

14 D. Flesch, S.-Y. Cheung, J. Schmidt, M. Gabler, P. Heitel, J. S. Kramer, A. Kaiser, M. Hartmann, M. Lindner, K. Lüddens-Dämgen, J. Heering, C. Lamers, H. Lüddens, M. Wurglics, E. Proschak, M. Schubert-Zsilavecz and D. Merk, *J. Med. Chem.*, 2017, **60**, 7199.